
Since January 2020 Elsevier has created a COVID-19 resource centre with free information in English and Mandarin on the novel coronavirus COVID-19. The COVID-19 resource centre is hosted on Elsevier Connect, the company's public news and information website.

# Nanomaterial-based sensors

13

*Fabiana Arduini*[1], *Stefano Cinti*[2], *Viviana Scognamiglio*[3] and *Danila Moscone*[1]
[1]Department of Chemical Science and Technologies, University of Rome "Tor Vergata", Rome, Italy, [2]Department of Pharmacy, University of Naples "Federico II", Rome, Italy, [3]Institute of Crystallography, Department of Chemical Sciences and Materials Technologies, Monterotondo Scalo, Rome, Italy

## 13.1 Introduction

Renaissance means new growth of activity or interest in something, especially art, literature, or music; nevertheless, we can stand this word in the science field as well. Among the multifarious branches of science, sensing is leading a renaissance era, thanks to the exploitation of cross-cutting technologies including nanotechnology, microfluidics and lab-on-chip, rational design, printing technology, and internet of things [1].

In particular, nanomaterials have been furnishing key instruments for easy engineering and fine-tuning unprecedented biosensing configurations based on recognition phenomena occurring at the nanoscale. Therefore, many nanomaterials have been widely exploited for the design of sensors and biosensors for several application fields. This established nanomaterial-based (bio)sensors as a hot topic, further confirmed by the fast growing of publications (Fig. 13.1).

Nowadays, emerging nanomaterials are available for customizing both electrochemical and optical (bio)sensors, thanks to their fascinating properties as strong absorption band in the visible region, high electrical conductivity, and good mechanical features. Indeed, several nanomaterials are exploited with custom-made properties and controlled nanodimensions, including spheres and particles [metal nanoparticles (NPs), magnetic beads, and quantum dots (QDs)], nanotubes, nanowires, nanorods, nanofibers, as well as nanocomposites, nanofilms, nanopolymers, and nanoplates.

A huge number of nanostructured (bio)sensors have been realized for many application fields exploiting different types of nanomaterials, including graphene, carbon nanotubes (CNTs), gold NPs (AuNPs), and nanomotors to name a few. Fig. 13.2 reports the trends of the last 10 years about the number of publications related to the use of the previously mentioned nanomaterials in the development of (bio)sensors, highlighting that graphene represents a rising star in the plethora of nanomaterials, while the use of CNTs remain almost constant. AuNPs have a slight

**Handbook of Nanomaterials in Analytical Chemistry. DOI: https://doi.org/10.1016/B978-0-12-816699-4.00013-X**

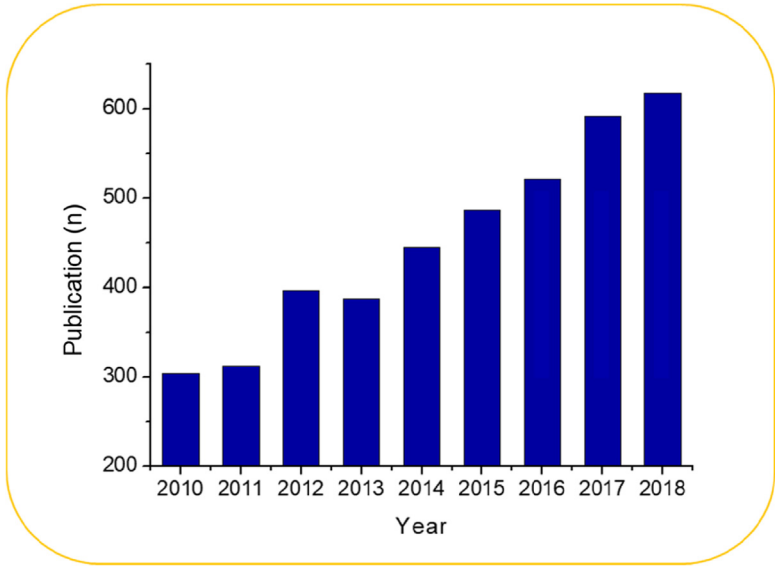


**Figure 13.1** Number of publications reported in Scopus with "nanomaterial and sensor" as keywords in the period 2010−18 (March 2019).

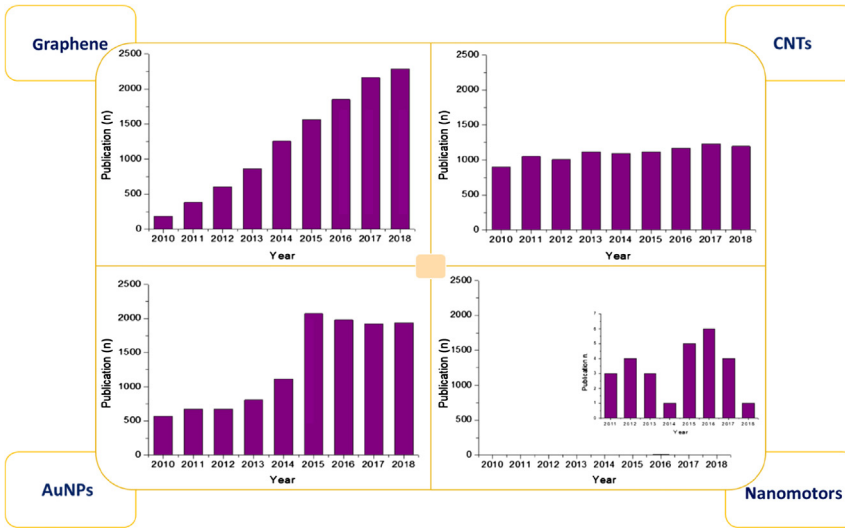


**Figure 13.2** Number of publications reported in Scopus with "graphene/carbon nanotubes/gold nanoparticles/nanomotors and sensor" as keywords in the period 2010−18. In case of nanomotors, the inset highlighted the low number of publications.

increase, and nanomotors are relegated at a proof-of-concept level. These astonishing outcomes obtained by scientists exploiting graphene in many fields, including sensor technology, resulted in the largest research initiative in the European Union (UE) with the "Graphene Flagship", *tasked with taking graphene from laboratories into the market with a €1 billion budget* [2].

If it is well established that nanomaterials entail inorganic materials, there is a new emerging vision, according to which biological materials as DNA and proteins can be considered as nanoscale entities being capable of folding in nanostructures [3–5]. As reported by *Nature Nanotechnology* journal "the ability of DNA to self-assemble into a variety of nanostructures and nanomachines is highlighted in a growing number of papers in *Nature Nanotechnology*. The appeal of DNA to nanoscientists is threefold: first, it is a natural nanoscale material; second, a large number of techniques for studying DNA are already available; and third, its ability to carry information can be exploited in the self-assembly process. DNA is also increasingly being used to organize other nanomaterials, and the related field of RNA nanotechnology is beginning to emerge" [6]. DNA is largely exploited as biological recognition elements (bioreceptors) in the design of biosensors, a branch of sensor technology. Beside DNA, enzymes are also used as biological recognition elements for catalytic detection as well as peptides and antibodies for affinity detection.

In this scenario, it is noteworthy that the arrangement of nanomaterials and biological materials plays a crucial role in the design of hybrid nanostructured analytical devices "with enhanced detection performance in terms of response time, higher storage/operational stability, resistance toward environmental conditions, improved selectivity, reduced sample volumes, and easy sampling" [7].

## 13.2 Graphene

Graphene is a high-quality 2D crystal (one-atom-thick) with unique electronic properties, becoming an unlimited promise in the development of field-effect transistors, photovoltaic devices, and biosensors. The astonishing features of this nanomaterial were recently praised by K.S. Novoselov in his Nobel lecture (December 8, 2010), stating that graphene is "more than just a flat crystal", which mimic massless relativistic particles, thanks to charge carriers. This crucial feature makes graphene a great candidate in the design of both electrochemical and optical (bio)sensors, being able:

1. to modify the electrochemical properties of an electrode and to work as label/loading agent for biomolecules and nanomaterials, thanks to its high surface area and easy functionalization, in the case of electrochemical transduction;
2. to provide fluorescence quenching at any wavelength by means of energy transfer in the case of optical transduction.

Therefore, depending on its multifarious configurations, graphene could be seen as a kaleidoscope in the realization of sensing tools with uncountable shapes, as largely described in the following subchapters.

### 13.2.1 Electrochemical graphene-based (bio)sensors

As a matter of fact, graphene is an excellent transducer material in biosensors, thanks to its propriety of high electron transfer and specific surface area. Graphene-modified screen-printed electrodes (SPEs) found applicable in many analytical sectors for revealing compounds ranging from clinical diagnosis to environmental pollution. Various graphene forms are available with graphene oxide (GO) and reduced graphene oxide (rGO) as the most used, or composites in combination with ZnO nanorods, CNTs, AuNPs, polyaniline, and pyrrole, just to name a few.

Graphene oxide nanosheets (GONs) were recently exploited as an SPE modifier in combination with titanium dioxide nanofibers (TNFs) to detect adenine by differential-pulse voltammetry (DPV) [8]. The authors underlined that the synergistic effect between GONs and TNFs, with an occurred decrease of overpotential and an increase of the peak current, resulted in a detection limit of 1.71 nM within two linear ranges (0.1−1 and 1−10 μM) in the presence of guanine as interferent.

rGO was also used as a network between ions and the electrode to design a disposable ion-selective electrode to selectively detect calcium [9]. In this case, the high graphene hydrophobicity prevented the formation of an aqueous layer inside the electrode avoiding drift instability, displaying a potential drift of only 14.7 $\mu V\ h^{-1}$ during continuous monitoring (20 h). This electrode (Fig. 13.3A) exhibited a Nernstian slope of 29.1 mV/decade, a linearity range of $10^{-5.6}$ to $10^{-1.6}$ M of $Ca^{2+}$ and a detection limit of $10^{-5.8}$ M. The same research group deposited rGO by one-step electrodeposition of the exfoliated GO sheets onto an ionic liquid-doped SPE for the detection of glucose by using glucose oxidase [11]. This graphene-modified electrode demonstrated the ability to reveal the enzymatic product hydrogen peroxide at a negative applied potential (−0.2 V vs Ag/AgCl) within a linear range from 0.15 μM to 1.8 mM. Therefore, glucose was detected with a sensitivity of 22.78 $\mu A\ mM^{-1}\ cm^{-2}$ and a detection limit of 1.0 μM, within a linear range up to 10 mM. The suitability of the biosensor was challenged in milk samples with satisfactory recovery values, demonstrating its aptness for glucose determination in real samples.

GO was similarly used in combination with ultrathin Au nanowires to modify SPEs for the development of an innovative 3D paper-based immunosensor to detect the tumor marker α-fetoprotein [10]. The presence of α-fetoprotein as low as 0.5 $pg\ mL^{-1}$ was evaluated by adding CuS nanoparticle-decorated graphene (CuS/GO) composites used as label of the signal antibodies, showing efficient electrocatalytic activity toward the reduction of $H_2O_2$ (Fig. 13.3B). In this work, graphene demonstrated to be able to augment the electrochemical performances of the SPE, as well as the antibody loading.

GO nanoplatelets electroactive properties were also recognized in a DNA electrochemical sensor for single-nucleotide polymorphism detection, based on the interactions between GO nanoplatelets and DNA strands [12]. The sensing mechanism was based on the different binding ability of single-stranded (ss) and double-stranded (ds) DNA toward GO nanoplatelets and the stronger ability of graphene to conjugate ssDNA with respect to dsDNA, demonstrating the inherently

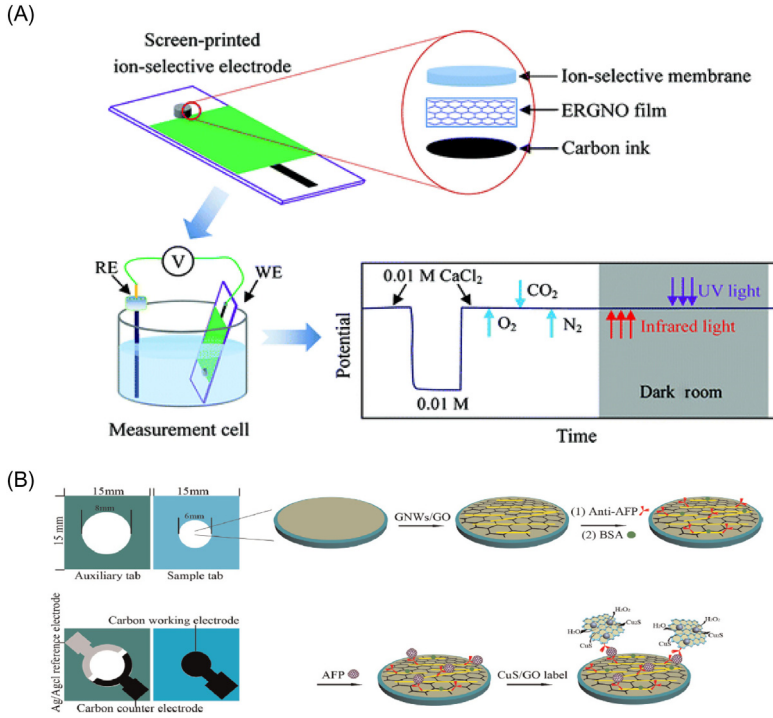


**Figure 13.3** (A) Ion-selective electrochemical sensor using graphene as the ion-to-electron transducer for calcium detection [9]. (B) Immunosensor for α-fetoprotein measurement designed by immobilizing the capture antibody onto the working electrode surface, previously modified by drop-casting GO and ultrathin gold nanowires. The binding with α-fetoprotein was evaluated by adding CuS nanoparticle-decorated graphene (CuS/GO) composites labeled to the signal antibodies [10].

electroactive property of GO. In this way, the detection at SPE of a noncomplementary target yielded a higher voltammetric signal than the complementary target at an SPE, because higher amounts of graphene were confined on the working electrode surface in the case of ssDNA.

### 13.2.2 Optical graphene-based biosensors

As aforementioned, graphene derivatives show multifarious characteristics, which can be exploited for the design of optical (bio)sensing systems, including the ability of fluorescence quenching at any wavelength by means of energy transfer. It is a matter of fact that the efficiency of this ability depends on the number of graphene layers as well as from their oxidation degree. The most used in optical (bio)sensors are oxidized graphene derivatives, which undergo a recombination of electron−hole pairs localized within an $sp^2$ carbon domain embedded within an $sp^3$ matrix, thus

resulting in characteristic photoluminescent properties. Indeed, it is possible to modulate the maximum fluorescence emission wavelength from the blue region to the near-infrared region by simply tuning the oxygen-containing moieties, the lateral size, and the oxidation degree [13].

These amazing features allowed to custom-make strategic DNA-based sensing principles based on effective interactions (hydrophobic and $\pi-\pi$ stacking interactions) between the hexagonal cells of graphene derivatives and the ring structures in nucleotides. The sensing mechanism of such biosensors is certainly elegant: an ssDNA labeled with a fluorescent probe is complexed with the graphene derivative, thus resulting in a quenched state when the analyte is absent. In the presence of the target analyte, the ssDNA/graphene complex is detached, hence recovering its fluorescence, as more weaker interactions between graphene and the nucleotide rigid structure occur (Fig. 13.4A) [14].

Different graphene derivatives have been exploited to set-up such sensing configurations, with graphene QDs and GO as the most common [13]. Morales-Narváez

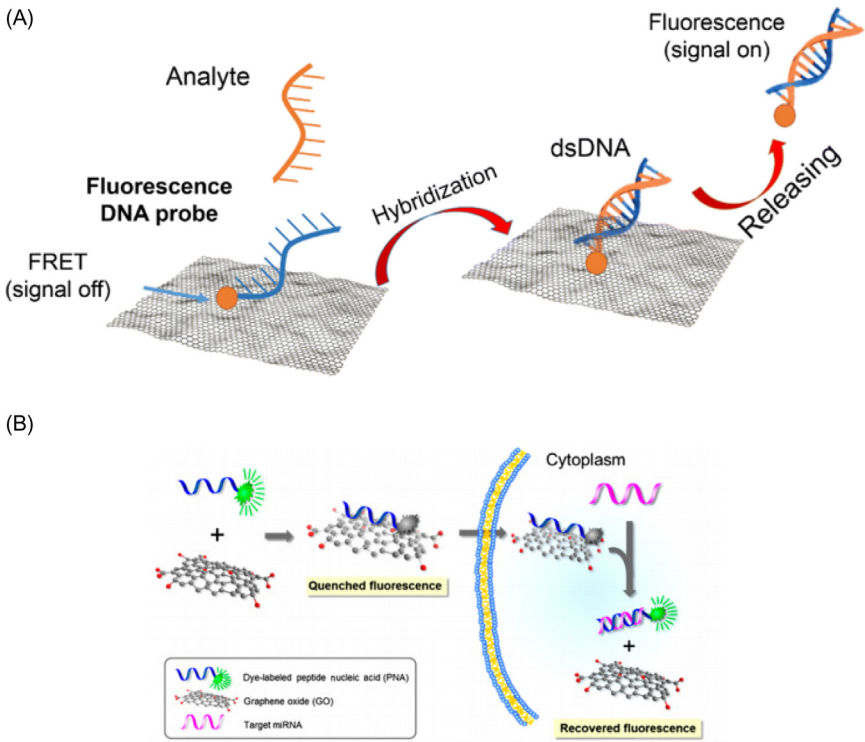


**Figure 13.4** (A) Scheme of graphene-based nanomaterials as a DNA biosensor with fluorescent detection [14]. (B) Scheme of strategy for a microRNA sensor based on graphene oxide (GO) and peptide nucleic acids (PNAs) for multiplexed microRNA sensing in vitro. The fluorescence signal is recovered when the fluorescent dye-labeled probes, initially adsorbed onto the surface of GO, detach from it and hybridize with a target microRNA [15].

and coworkers used antibody/QD (Ab-QD) probes and GO to design a pathogen-detection microarray [16]. This sensing principle is based on the energy-transfer phenomenon that occurs between photoexcited QDs and GO when in close proximity. In the absence of the pathogen, the Ab-QD probes extensively interact through $\pi-\pi$ stacking with GO, which quenches their fluorescence. When the pathogens are selectively captured by the Ab-QD probes, they fluoresce when excited with a laser, since a weaker interaction occurs with GO that, in this configuration, is not more capable of strong fluorescence quenching. As a model pathogen to test the system, *Escherichia coli* O157:H7.16 was used, while QDs were (core-shell) CdSe@ZnS QDs functionalized with streptavidin. This biosensing approach led to a highly specific and sensitive analysis, noticeable up to 10 CFU $mL^{-1}$ in standard buffer and 100 CFU $mL^{-1}$ in bottled water and milk.

Ryoo and coworkers [15] described the use of GO for the development of an optical biosensor to detect microRNAs exploiting peptide nuclei acids (PNA), highlighting the advantages of graphene as high loading capacity nanomaterial for bioreceptor immobilization. In particular, GO was used both as scaffold for peptide nucleic acid and as a quencher for the fluorophore attached to the PNA probe (Fig. 13.4B). After the addition of the target, the labeled PNA was able to emit fluorescence in a concentration-dependent manner monitoring target microRNAs in the picomolar range.

## 13.3 Carbon nanotubes

In 1991, a letter of Iijima was published on *Nature*, reporting the synthesis of nanometer-size and needle-like tubes of carbon, namely helical microtubules of graphitic carbon, that now we call CNTs. CNTs came across notable interest in chemistry, physics, and material science since their discovery in 1991, own to their 1D structure and unique properties [17]. These tubular structures are composed by $sp^2$ carbon units and can stand principally as single-walled CNTs (SWCNTs) and multi-walled CNTs (MWCNTs). Many research articles have been published entailing CNTs for several applications such as microelectronic circuitry, biological systems, and sensing devices also coupled with other nanomaterials, compounds, or/and biocomponents [18].

### 13.3.1 Electrochemical carbon nanotube-based (bio)sensors

The copious features of CNTs, as the electrocatalytic properties own to edge defect sites and metal impurities, combined with the high surface area, suitable to immobilize nanomaterials and/or biocomponents, have been widely exploited to develop electrochemical (bio)sensors. Indeed, in the years comprised between 1991 and 2010, CNTs played a noticeable role in sensor design, afterward losing their leading position because tarnished by graphene.

As mentioned above, CNTs were principally used in combination with other nanomaterials, as in the case of Dong et al. [19], which developed a glassy carbon

electrode modified with a nanocomposite constituted of MWCNTs−$CeO_2$−Au NPs for methyl parathion detection, with a limit of $3.02 \times 10^{-11}$ M. This nanocomposite was able to perform the solid-phase extraction of the herbicide, thanks to the exceptional adsorption properties of MWCNTs, resulting in high sensitivity. Moreover, because of the presence of $CeO_2$ and AuNPs, a high surface area and a special catalytic activity were provided, with a great sensitivity improvement when methyl parathion was detected in river and soil samples.

MWCNTs were also joined with GO sheets by Huang et al. [20] to release an interesting hybrid nanocomposite used to modify glassy carbon electrodes for the detection of $Pb^{2+}$ and $Cd^{2+}$ with a detection limit of 0.2 and 0.1 $\mu g\ L^{-1}$, respectively (Fig. 13.5A). This nanocomposite was characterized by an excellent conductivity and a good water-solubility, overcoming respective deficiencies, since the hydrophilic GO sheets could load CNTs through $\pi-\pi$ stacking interactions, overcoming the solubility problem, while the presence of CNTs suppresses the aggregation between GONs.

CNTs also showed high capability for bioreceptor immobilization, enhancing the biomolecule loading as well as the electrochemical analytical performances, as demonstrated by Vicentini et al. [21]. The authors immobilized tyrosinase enzyme on CNTs using their carboxylic moieties. In detail, tyrosinase was covalently immobilized onto CNTs by means of (1-ethyl-3-(3-dimethylaminopropyl)-carbodiimide) and *N*-hydroxysuccinimide, for catechol detection with a detection limit of 0.58 μM (Fig. 13.2B).

### 13.3.2 Optical carbon nanotube-based (bio)sensors

The brilliant exclusive optical features of CNTs have gained huge attention among researchers in the development of optical biosensors for the detection of several analytes of biomedical and agro-environmental interest. Indeed, such nanomaterials possess peculiar characteristics that can be tuned for the different optical transductions, including luminescence, fluorescence, and color changes, as well as extended wavelength range of emission from 700 to 1400 nm, high photostability, low autofluorescence, and deep penetration capability in skin for in vivo imaging among others [22].

CNTs are rolled-up cylinders of carbon monolayers (graphene), which can be chemically custom-made in such a way that bioreceptors can be accommodated in ideal environments to enhance their robustness as well as their sensitivity and selectivity toward target molecules [23].

The most important optical sensing mechanisms exploiting CNTs are:

1. Fluorescence: change of the fluorescence spectrum due to the interaction between analyte and SWCNT/wrapping (intensity or wavelength shift);
2. Quenching: proximity quenching of other (organic) fluorophores; and
3. Raman scattering: CNTs are used as a tag exhibiting extremely high Raman scattering.

Several biosensors using CNTs have been described in the literature toward different target analytes from DNA [24] to oxygen reactive species [25], hydrogen

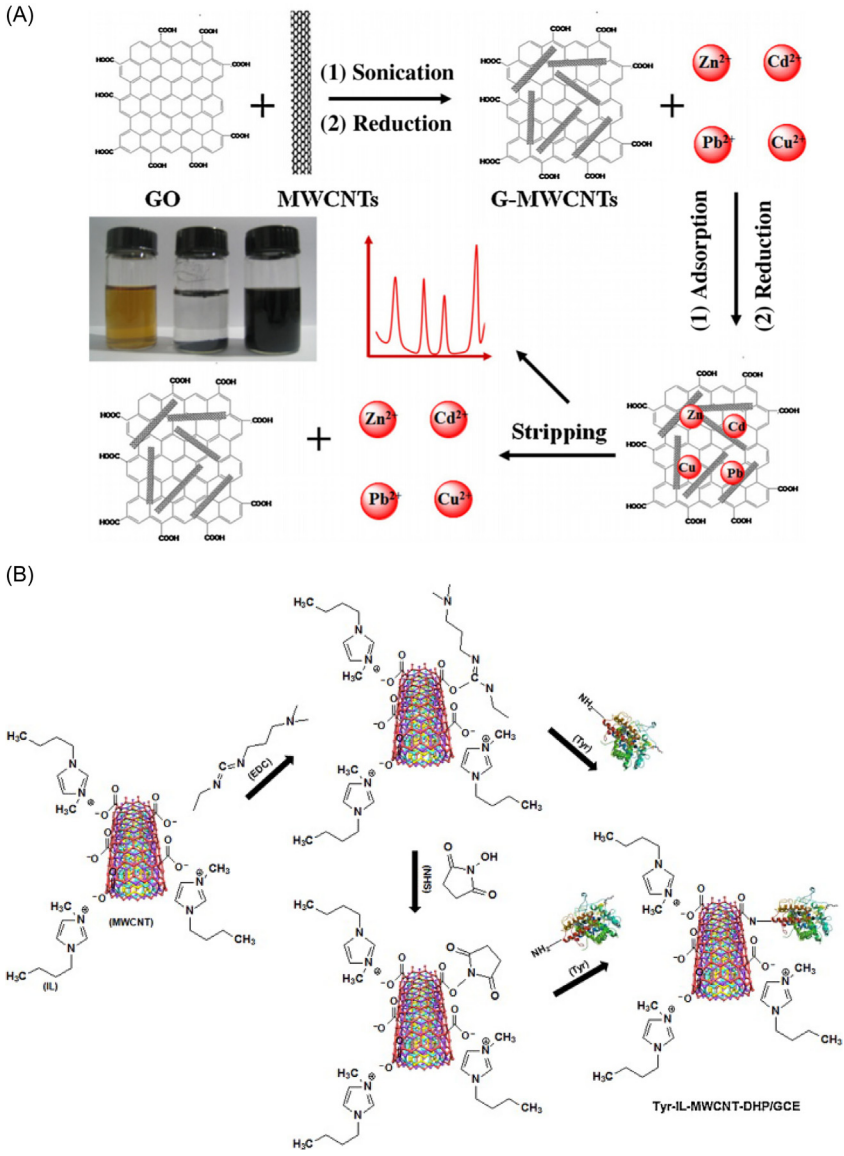


**Figure 13.5** (A) Scheme of GO and MWCNTs nanocomposite and its application for heavy metal detection [20]. (B) Scheme of the reaction used to immobilize tyrosinase enzyme on MWCNT [21].

peroxide [26], nitric oxide [27], proteins [28], and small molecules as ATP [29]. Many CNT-based biosensors have been also setup for glucose monitoring in diabetic patients because of CNTs high suitability in the design of continuous implantable diagnostic tools where high sensitivity, tissue transparency, and no

photobleaching are required. Yoon et al. [30] covalently conjugated the periplasmic glucose-binding protein from *E. coli* with carboxylated poly(vinyl alcohol)-wrapped SWNTs, leading to allosterically controlled optical transduction by reversible exciton quenching in response to glucose. Glucose-binding protein is characterized by two domains linked by a "hinge" region; it binds the sugar with very high specificity undergoing a conformational change in which the two domains close around the glucose. This actuation resulted in changes of the polymer−SWCNT interaction, ultimately causing a highly selective and reversible SWCNT fluorescent quenching, proportional to the glucose concentration. Changes in fluorescence emission of glucose-binding protein/SWNTs were analyzed at different glucose concentrations, over a long observation time ($>60$ h), thanks to the photostability of SWNT.

A similar approach was exploited by Ahn et al. to study the interaction mechanisms among proteins [31]. In detail, they used CNTs as optical sensors for the label-free detection of protein−protein interactions where each nanotube was encased within a chitosan polymer wrapping modified with nitrilotriacetic acid moieties (Fig. 13.6). After $Ni^{2+}$ chelation, NTA−$Ni^{2+}$ complexes work as proximity quenchers, modulating the intrinsic SWCNT fluorescence intensity as a function of distance from the SWCNT surface. The $Ni^{2+}$−NTA group binds to any capture protein, which possesses a hexahistidine tag. Upon target binding to the capture protein, a variation of $Ni^{2+}$-SWCNT distance occurred, allowing for the evaluation of protein binding by means of fluorescence intensity changes.

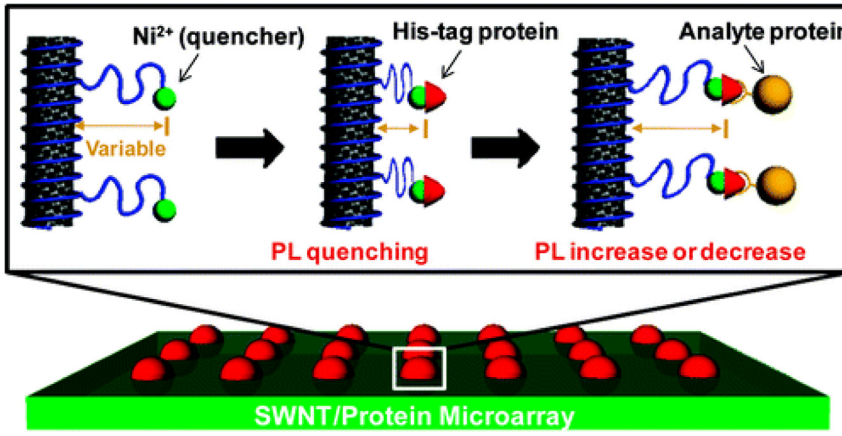


**Figure 13.6 Schematic of the SWCNT array and the signal transduction**. NTA-bound $Ni^{2+}$ ions act as proximity quenchers of the nanotube fluorescence. Upon binding of a his-tagged capture protein, the distance of the ion from the SWCNT surface decreases, resulting in a fluorescence-quenching response. Upon binding of an analyte protein to the his-tagged capture protein, a further fluorescence modulation occurs, allowing for direct detection of the binding event [31].

As evidenced, obvious advantages of CNTs make them suitable candidate in the design of optical biosensors. Among others, CNTs' different chiralities allow to configure multiplexing platform since every SWCNT could be used as a single color. However, this diversity can also be considered as a concern, since so far ensembles of different chiralities, length, and impurities might decrease sensitivity and selectivity. The lower fluorescence quantum yield can be also considered a drawback if compared with high quantum yield fluorophores, as for example QDs; thus many other nanomaterials are gaining much attention in the last years, as a replacement to CNTs.

## 13.4 Other carbon-based materials

It is noteworthy that the properties of one and two-dimensional (2D) graphitic materials, such as CNTs, graphene, and other carbon nanomaterial as carbon nanofibers (CNFs) have received increased attention due to their physical and chemical properties not available in other materials, such an interesting molecular structure, high surface area for bioreceptor loading, size-tunable emission, narrow and symmetric photoluminescence, broad and strong excitation spectra, strong luminescence, and robust photostability. Thanks to these fascinating properties, these carbon nanostructures have been extensively used for the development of electrochemical and optical (bio)sensors.

### *13.4.1 Other carbon-based materials in electrochemical biosensors*

Among the most famous carbon-based materials namely graphene and CNTs, carbon black (CB) is a carbon nanomaterial that has recently attracted a huge attention by scientists thanks to its cost-effectiveness as well as outstanding electrochemical properties. Before 2010, few articles have been reported for the application of CB as electrode modifier for analyte detection in solution. Only after 2010 there was a relevant growth of publication number describing CB as electrode nanomodifier. Our group highlighted the mesmerizing electrochemical characteristics of CB in the ink/paste as well as in modifying electrodes by drop-casting to reveal many analytes as catechol, hydrogen peroxide, nicotinamide adenine dinucleotide (NADH), and thiocholine [32–35]. Our results were validated by other groups: Compton's group [36] reported the gain of using CB over the more specialized MWCNTs in terms of sensitivity toward the detection of nicotine by adsorbitive stripping voltammetry, because the presence of CB allowed higher current responses for nicotine oxidation at lower potentials. Pumera's group [37] demonstrated that CB is more suitable than the thermally reduced GO, being cheaper and not requiring any chemical and physical treatment before use. Fatibello-Filho's group [38] as well as Evtugyn's group [39] successfully used CB-modified electrodes for the detection of different analytes. Arduini et al. [35] reported a miniaturized and disposable

electrochemical sensor for phenolic compound detection constructed by modifying the working electrode surface of SPEs with CB dispersion (Fig. 13.7A). This sensor showed higher sensitivity and better resistance to fouling than the bare SPE, displaying the suitability of CB as an excellent electrode nanomodifier. Catechol, gallic acid, caffeic acid, and tyrosol were detected by square-wave voltammetry with detection limits of 0.1, 1, 0.8, and 2 μM, respectively.

Other recently used nanomaterials with peculiar features are magnetic carbon structures, starting from spheres (CSs) to more elongated structures as tubes and fibers, with nano- and microsize. Arduini and colleagues [40] combined CSs with SPEs highlighting their electrochemical effectiveness toward the detection of several species, that is, ferricyanide, ascorbic acid, dopamine, cysteine, serotonin, and NADH (Fig. 13.7B). The presence of iron nuclei within the carbonaceous lattices, besides improving the electrochemical performances of the printed electrodes, might confer these CS-based structures a future application in the field of remediation/sensing. In addition, this magnetic material was used for collecting the sample (e.g., ferricyanide) and measuring it on the working electrode surface by cyclic voltammetry.

### 13.4.2 Other carbon-based materials in optical biosensors

Many optical biosensors entail fluorescence transduction based on Förster resonance energy transfer (FRET), which consists in the transfer of energy from a photoexcited energy donor to a close energy acceptor. To this aim, carbon nanomaterials are good candidates for biosensor configuration as smart quenchers. Morales-Narváez and coworkers [41] explored the ability of different carbon nanomaterials as quencher in comparison with the most used QDs for FRET measurements. In this regard, the authors exploited QDs as donors and graphite, CNTs, CNFs, and GO as energy acceptors of FRET from QDs. The responses of the explored carbon-based materials as acceptors of QD FRET donors in the proposed platform are displayed in Fig. 13.8. They observed that graphite was a weak acceptor for spots deposited from high concentration suspensions ($0.5-1$ mg $mL^{-1}$), while for thinner films at graphite lower concentrations ($0.125-0.25$ mg $mL^{-1}$), graphite becomes a strong acceptor. Both CNT and CNF in general behave as stronger acceptors in comparison to graphite, whereas, as observed, the strongest quenching is caused by GO at all the studied concentration values (from 0.125 to 1 mg GO $mL^{-1}$).

A recent example of optical biosensor based on carbon nanomaterials was described by Wang and colleagues for the detection of thrombin by exploiting aptamers and FRET [42]. In detail, poly(acrylic acid) functionalized upconverting phosphors were covalently tagged with a thrombin aptamer, bound to the surface of carbon NPs through $\pi-\pi$ stacking interaction. The energy donor and acceptor were taken into close proximity, providing quenching of upconverting phosphors. The presence of thrombin allowed for quadruplex structure of the aptamer resulting in the increasing of the distance between acceptor and donor, blocking the FRET process, restoring the fluorescence in a thrombin concentration-dependent manner.

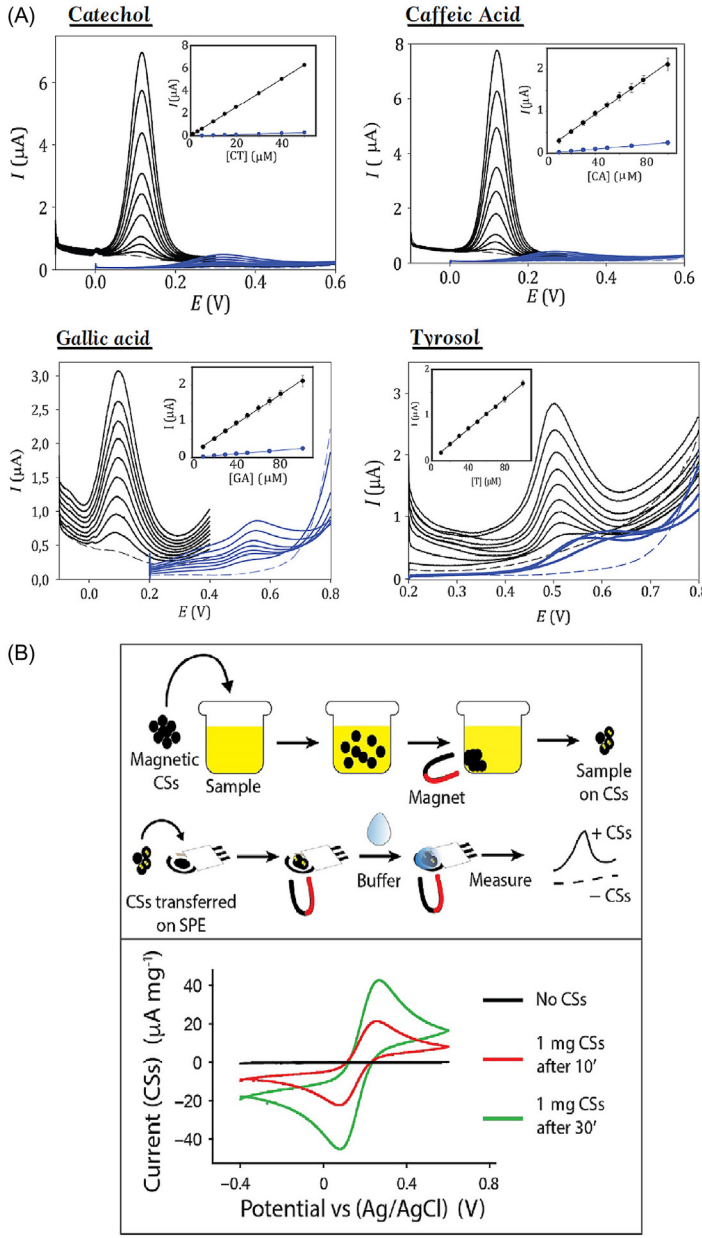


**Figure 13.7** (A) Square-wave voltammetry using bare SPE (***blue*** line) and SPE modified with CB (*black* line) in absence (*dashed* line) and in the presence of different concentrations (*continuous* line) of catechol, caffeic acid, gallic acid, and tyrosol [35]. (B) Schematic representation of the experimental path followed to collect ferricyanide on the aggregate CSs and release the same molecule on a printed electrode, that is, SPE. Electrochemical detection by using a bare SPE without CSs aggregate (*black* line) and in presence of 1 mg of CSs aggregate immersed for 10 (*red* line), and 30 (*green* line) min in a 3-mL solution containing 10 mM ferricyanide [40].

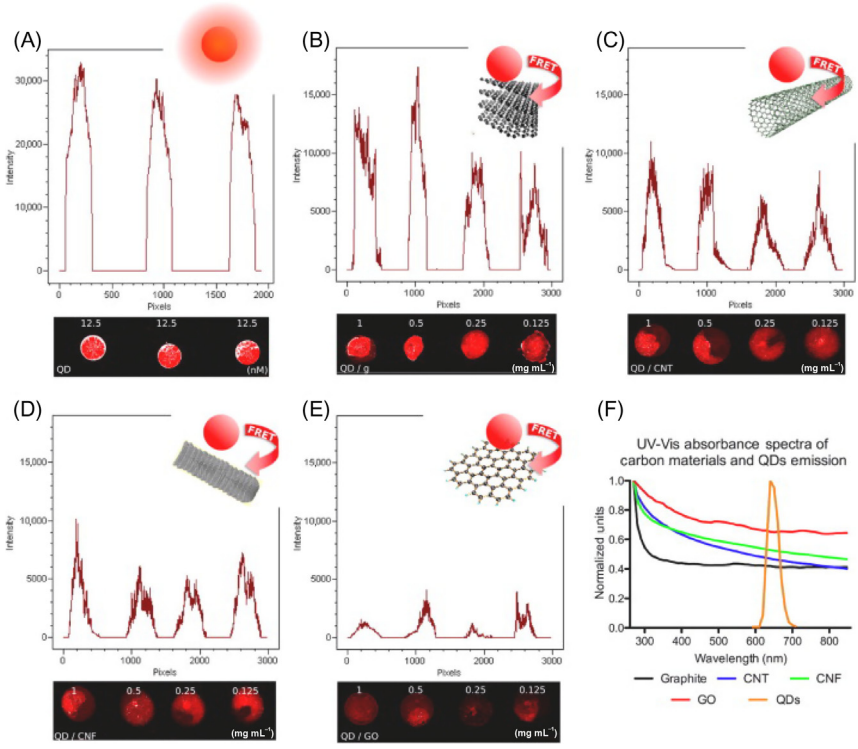


**Figure 13.8** Responses of four carbon-based materials as acceptors of QDs FRET donors in the solid phase and their UV−Vis spectra. Graphs show fluorescent intensity profile of the spots. (A) Unquenched QDs (*blank*). (B) QD quenching by graphite. (C) QD quenching by carbon nanotubes (*CNTs*). (D) QD quenching by carbon nanofibers (*CNFs*). (E) QD quenching by graphene oxide (*GO*). Carbon-based material concentration: 1, 0.5, 0.25, 0.125 mg $mL^{-1}$ in dimethylformamide (DMF) (from *left* to *right* respectively). QD concentration: 12.5 nM in PBS. (F) UV−Vis absorbance of the studied carbon materials and QD emission (excitation wavelength, 630 nm) [41].

The sensor provided a linear range from 0.5 to 20 nM for thrombin with a detection limit of 0.18 nM in an aqueous buffer.

## 13.5 Non-carbonaceous nanomaterials

Beyond the use of carbonaceous-based entities such as graphene, nanotubes, CB, fullerene, etc., creating nanostructures starting from noble metals has been widely adopted in producing both electrochemical and colorimetric sensing platforms. However, many other nanomaterials can improve the performance of sensing devices such as inorganic crystals, oxides, and semiconductors, which can be

synthesized at nanosized level to reveal their tremendous enhancement of proprieties while detecting traces of analytes in complex matrices such as surface waters, blood, urine. Prior to analyzing the various applications related to the use of nanomaterials, it should be noted that many of them can be used in a ubiquitous way. For example, AuNPs can be used for the development of colorimetric assays due to their size-dependent plasmonic band and also for the realization of electrochemical platforms by exploiting their high surface area and electrocatalysis [43].

In next section, some of the successful applications of these nanosized boosters are reported.

### 13.5.1 Non-carbonaceous nanomaterials electrochemical (bio)sensors

#### 13.5.1.1 AuNPs

Recently, AuNPs have been used to develop screen-printed paper strips for the electrochemical detection of ss- and ds-DNA sequences related HIV in serum samples [44], as shown in Fig. 13.9A. In this work, two kind of paper-based substrates, namely filter and copy papers, have been evaluated toward the realization of an affordable device capable to detect targets in few microliters of undiluted serum samples. The AuNPs have been obtained by making an Au precursor salt reacting with a reductant (sodium borohydride) and a capping agent (sodium citrate). However, it should be considered that the synthesis of the final $\sim$20 nm NPs needed very clean glassware (in fact, aqua regia and piranha solution have been used for cleaning). The role of AuNPs was dual: they served as anchor points for the attachment of the thiol-extremity of the DNA probe, and they produced an obvious improvement of the electrochemical properties compared to unmodified graphite-based printed electrodes. AuNPs allowed, at a very low cost of production, to reach detection limit of 3 and 7 nM, respectively, for ss and ds sequences. In comparison with the classical approaches, that involve the use of Au macroelectrode, the use of AuNPs for DNA sensing is highly recommendable especially in terms of surface-to-volume ratio.

The use of AuNPs has been also adopted for the analysis of heavy metals in environmental context such as the detection of arsenic in surface waters [47] and mercury in soil [48]. Clear advantages must be attributed to the combined presence of AuNPs and CB. The latter allowed increasing the spreading of AuNPs on the top of the SPE area, thus augmenting the available area for detecting the metals. Arsenic and mercury have been detected, respectively, down to 0.4 and 3 ppb as detection limits. The extremely high portability of the platforms permitted to carry out the measurements directly on-site, reducing costs and time-consuming procedures of laboratory-based settings.

However, the use of AuNPs should not only be linked to the modification of the electrode's surface. In fact, AuNPs can also be applied as electrochemical label. The group of Merkoçi developed a new methodology for the isothermal amplification of Leishmania DNA using magnetic beads coupled to AuNPs [49]. The

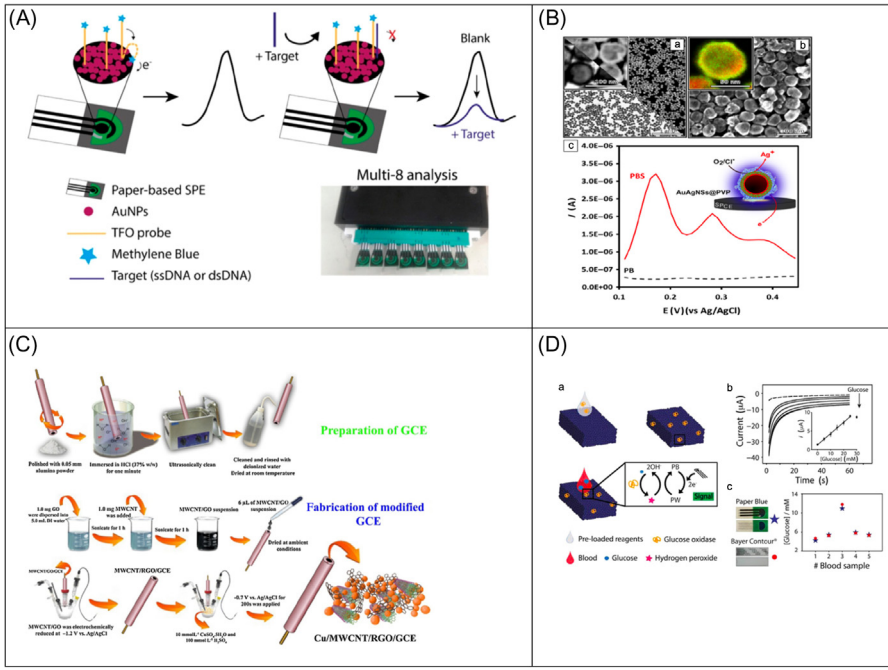


**Figure 13.9** (A) Schematic representation of the paper-based E-DNA platform for the detection of single- and double-stranded DNA targets. The measurements have been carried out with a multi-8 reader, by using one-shot SPE for each concentration of target [44]. (B) TEM micrographs of AuAg NSs composed, SEM of AuAg NSs surface characterization, comparison of differential-pulsed voltammetries (*DPVs*) of AuAg NSs in different buffers. In the absence of chlorides in the matrix, no Ag corrosion is possible and therefore no stripping detection can be carried out (Permission from [7]); (C) Preparation of GCE and fabrication of modified GCE with CuNPs-multiwalled carbon nanotubes-reduced GO [45]. (D) Development and measurement scheme of the blood glucose biosensor on paper Blue. Amperometric detection of increasing concentration of glucose (0−30 mM), applying −0.1 V. Inset: calibration curve of glucose in the range 0−30 mM (measurements have been carried out in 0.05 M phosphate buffer, pH 7.4); Paper Blue versus Bayer Contour for blood glucose determination [46].

presence of magnetic beads allowed to purificate/concentrate the analyte, while AuNPs were used both to label the oligonucleotide primers and to enhance the electrochemical signal for the rapid quantification of the DNA on screen-printed carbon electrodes. The presence of AuNPs displayed an electroactive role toward the hydrogen evolution reaction after the addition of acid, and this strategy yielded the quantification of less than one parasite per microliter of blood. The adoption of this inorganic label allowed to achieve a good stability in terms of shelf-life of the primer/AuNPs adduct, that in fact arrived up to 8 weeks when stored at 4°C and in dark condition.

### 13.5.1.2 AgNPs

Although the use of AuNPs for the development of electrochemical platforms represents the majorly adopted choice, AgNPs are also used for the realization of sensors and biosensors. However, due to the susceptibility of Ag to be oxidized in presence of halide ions when a slightly positive potential is applied, especially in presence of chloride, its application as an electrode modifier does not represent the first choice because its oxidation might hide the peak corresponding to the species of interest. On the contrary, the use of AgNPs is particularly effective when an electrochemical label is needed. Many examples are reported within the field of electrochemistry. For instance, AgNPs together with graphene have been used to develop a novel trace label for the development of a clinical immunosensor for avian influenza virus H7 [50]. In order to produce a stable adduct, a chitosan solution has been added to provide carboxylic groups (after NaOH treatment) for the conjugation with H7-polyclonal antibodies, making a biohybrid conjugate. Taking advantage of the high surface-to-volume ratio of graphene, a high amount of AgNPs has been immobilized, and allowed to improve the sensitivity of the final platform by detecting the virus with a detection limit of 1.6 pg $mL^{-1}$ and a four-orders linearity range (up to 16 ng $mL^{-1}$). In addition, the bioconjugate retained more than 90% of its initial activity after a storage period of 1 month in phosphate-buffered saline solution.

Beyond this, the use of AgNPs as electrochemical label has been recently demonstrated in combination with Au. Russo et al. [51] took advantage of a novel class of nanomaterial, namely hollow AuAg nanoshells (NSs), to detect *E. coli* and *Salmonella typhimurium* at a screen-printed carbon-based electrode. The determination of bacteria is due to non-specific affinity interactions between bacteria's walls and AuAg NSs surface. The electrochemical mechanism is because if the AuAg NSs are exposed to a high concentration of halides and dissolved oxygen, $Ag^{+}$ cations can be produced by galvanic corrosion without compromising the particles' structural stability, and anodic stripping analysis can be performed. This proof-of-concept approach allowed reaching high sensitivities down to $10^2$ CFU $mL^{-1}$ in only 10 min. However, this assay was not able to distinguish and quantify different bacterial strains in complex mixtures and the presence of interfering species such as copper and mercury, lead to an electrochemical quenched effect due to suspected formation of alloys and amalgams between these cations ($Cu^{2+}$, $Hg^{2+}$) and the noble metals, Au and Ag, constituting the NSs, as reported in Fig. 13.9B.

The use of AgNPs has been also adopted for the rapid detection of another human pathogen, the *Staphylococcus aureus* [52]. In this work, AgNPs were conjugated to an anti-*S. aureus* aptamer to be integrated into an immunoassay platform. Briefly, a biotinylated primary anti-*S. aureus* aptamer was fixed onto streptavidin-coated magnetic beads that served as the capture agent. Subsequently, a second anti-*S. aureus* aptamer (conjugated to AgNPs by means of S−Ag covalent bond) was allowed to form a sandwich structure with the bacterium, and the electrochemical signal of Ag ions was carried out by means of anodic stripping voltammetry (in strong acidic conditions). The electrochemical immunosensor displayed a dynamic range comprised between 10 and $10^6$ CFU $mL^{-1}$ with a detection limit calculated

($S/N = 3$) equal to 1 CFU $mL^{-1}$. Authors claimed that the sensitivity of the developed assay is strictly dependent on the Ag ions released by each NP, that is, $10^6$ ions from a 40-nm particle. In addition, the use of AgNPs instead of AuNPs should be preferred also because the electrochemical redox reactions of Ag occur at lower potentials with respect to those needed by colloidal Au.

### 13.5.1.3 Cu nanoparticles and Pt nanoparticles

Within the electrochemical development of sensors and biosensors, though the role of Au and Ag for making smart NPs represents the majority of applications, other metals can be obtained in form of NPs/nanocomposites such as copper and platinum. Even if their usage is not spread as well as the previous ones, some nice applications have been reported in literature. CuNPs have been used to modify the electrodic surface for the detection of nitrite and nitrate ions in food and beverages samples. The authors developed a sensing tool by electrodepositing CuNPs onto a layer composed by multiwalled CNTs-reduced GONs [45] (Fig. 13.9C). The presence of CuNPs was necessary to carry out nitrite and nitrate detection at the glassy carbon electrode. In addition, the combination between carbonaceous material and copper allowed reaching a two-fold enhancement of the platform sensitivity. Both the ions were detected by square-wave voltammetry within the 0.1−75 μM range with detection limits of 20 and 30 nM, respectively, for nitrate and nitrite ions. An experimental issue demonstrated the effect of chloride ions in solution, similar for the simultaneous determination of nitrite and nitrate: their presence might form a surface layer onto the modified electrode, altering the double layer characteristics; to avoid this, an Ag-impregnated filter could be used to remove the excess of chloride ions.

The use of CuNPs has been also used to mimic the role of an enzyme. In fact, metal-organic frameworks (MOFs) have been used as an envelope for Cu NPs for nonenzymatic glucose sensing in alkaline media [53]. The encapsulated CuNPs in organic zeolitic imidazolate framework have been adsorbed onto a SPE. The presence of MOFs allowed to enhance the stability of CuNPs, preventing their dissolution and agglomeration during the electrocatalytic analysis. This effect was also confirmed through a comparison with a layer-by-layer approach, indicated by the authors as Cu-on, instead of Cu-in, that is, encapsulation. The use of transition metals such as copper was also convenient because of the easier controllable synthesis, higher activity and lower cost, if compared to Au-based platforms. The limit of detection was calculated to be 2.76 μM on the basis of $S/N = 3$, and the linearity was observed up to 0.7 mM. In addition, this device was successfully compared with a commercial glucometer (One Touch Ultra, LifeScan), achieving a good agreement.

Another example of electrocatalytic metal encapsulation is represented by platinum. With a similar strategy, platinum NPs (PtNPs) have been encapsulated into MOFs to detect the activity of telomerase [54]. It was detected in cancer cells following the electrocatalysis of PtNPs in the presence of $NaBH_4$ oxidation in alkaline media. To perform the detection, a capture probe has been linked onto the

PtNPs-MOF adduct, and it has been able to recognize DNA sequences related to telomerase extract. The electrochemical signal is produced following the addition of $NaBH_4$ because its oxidation involves a maximum of eight electrons: this effect is much higher in respect to those involving one- or two-electron process. A traditional glassy carbon electrode was adopted to realize this biosensor, which showed a dynamic correlation with the telomerase activity from 500 to $10^7$ cells $mL^{-1}$, and the activity calculated in a single cell was equal to $2 \times 10^{11}$ IU.

#### 13.5.1.4 Inorganic nanoparticles

Not only metallic NPs have been used to enhance the electrochemical performance of sensors and biosensors. Plenty of nanomodifiers, including inorganic crystals, metal oxides, etc. have been used to develop the "right" platform. In the electrochemical field, one of these is without doubts the Prussian Blue also known as "artificial peroxidase" for its selectivity toward hydrogen peroxide [55]. The use of Prussian Blue (ferric hexacyanoferrate) has been widely adopted toward the determination of hydrogen peroxide, also in biosensing architectures involving the use of oxidase enzymes, that is, alcohol, glucose, lactate, cholesterol, etc. [56–58]. In particular, a novel approach has been recently used to produce Prussian Blue NPs: the cellulose network of filter paper has served as a reactor for fabricating these NPs [46]. Briefly, the structure of a common filter paper has been used to synthesize prussian blue nanoparticles (PBNPs) starting from their precursors without the need of any external power source and/or reducing agents. The synthesis has been entirely attributed to the composition and structure of paper, and NPs of $\sim$20 nm have been produced. This approach represented the first paper-based mediated synthesis of NPs and the so-called "Paper Blue" has been applied toward the detection of glucose in whole blood. This biosensor was capable to detect glucose linearly up to 25 mM, and the presence of Prussian Blue NPs highlighted a high selectivity even in the presence of common potential blood interferents, for example, ascorbic acid, uric acid, and acetaminophen. Moreover, this paper-based biosensor was positively compared with the commercially available strips (Bayer Contour) with a correlation of 0.987, as displayed in Fig. 13.9D.

Beyond the activity toward hydrogen peroxide, PBNPs have been also used to detect thiols. In particular, combined with CB, for the development of organophosphate pesticide biosensor [59]. In this case, the synthesis of PBNPs was performed directly onto CB that acted as nucleating sites for NPs' formation. After the nanocomposite was produced and purified, it was mechanically mixed within the carbon ink and screen-printed onto a waxed filter paper. The pesticide was detected by taking advantage of a dual electrochemical measurement, in parallel, of butyrylcholinesterase (BChE) enzyme activity toward butyrylthiocholine with and without pesticide (the enzyme inhibitor). This all-in-one biosensor allowed to detect the enzymatic inhibition caused by the presence of a model analyte, that is, paraoxon, linearly up to 25 $\mu g\ L^{-1}$ with a detection limit found equal to 3 $\mu g\ L^{-1}$.

Another interesting biosensing approach has been reported by Rivas et al. while developing an aptasensor for ochratoxin A (OTA) [60]. This electrochemical

platform has been obtained by electropolymerizing a film of polythionine onto a carbon SPE, followed by the assembly of iridium oxide NPs ($IrO_2$NPs). The immobilization of the OTA-recognition aptamer was achieved through the electrostatic interactions produced as a consequence of the attraction between the negatively charged citrate groups surrounding $IrO_2$NPs and the positively charged amino groups of the amino-modified aptamer. This platform allowed to develop a label-free tool based on impedimetric detection of OTA in the interval between 0.01 and 100 nM with a detection limit of 14 pM.

## 13.5.2 Noncarbonaceous nanomaterials optical (bio)sensors

### 13.5.2.1 AuNPs

A great possibility of using AuNPs in developing colorimetric assay, but even other metal-based nanomaterials, is attributable to the fact that the color of colloids depends on their shape and chemical environment. For instance, the use of 1-(2-mercaptoethyl)-1,3,5-triazinane-2,4,6-trione (MTT)-functionalized AuNPs allowed detecting nitrite ions by exploiting the "molecular bridge" among the different MTT-AuNPs [61]. The presence of $NO_2^-$ ion was capable to promote interactions between NPs, provoking the red wine color of MTT-AuNPs changing into the purple-gray color. The absorbance of the plasmonic band shifted from 535 to 790 nm, and it could be attributed to the closer contact among MTT-AuNPs, due to aggregation. The analytical performance was satisfactory: the linear regression of the calibration curve showed a good correlation coefficient ($R^2 = 0.9737$), the detection limit was calculated equal to 1 $\mu g\ mL^{-1}$, and it was within the legal limits established by US EPA and WHO for drinking water. It should be noted that the presence of common interfering species such as fluoride, chloride, bromide, phosphate, sulfate, and nitrate ions, did not affect the nitrite analysis.

Another elegant application of AuNPs has been reported toward the colorimetric detection of organophosphorous pesticides: the scheme of detection has been based on the enzymatic hydrolysis reaction of acetylcholinesterase (AChE) and the dissolution of AuNPs in $Au^{3+}$/cetyltrimethylammonium bromide (CTAB) [62], as reported in Fig. 13.10A. The dissolution of AuNPs represents a new mechanism: in fact, they can be dissolved by a mild oxidant in the presence of CTAB, exhibiting an evident shift from red to colorless. In this case, when the enzymatic substrate (acetylthiocoline) is converted by AChE, the by-product thiocholine protects AuNPs from dissolution; instead, when the inhibitor is present, the enzymatic reaction does not occur properly, AuNPs are oxidized to $Au^{3+}$/CTAB and the color changes from red to pink/colorless. Under the optimized conditions, parathion (the model inhibitor) was detected down to 0.7 ppb and the presence of small amount of salt (5 mM NaCl) did not affect the stability of method.

Beyond these approaches, the use of AuNPs represents the "gold standard" in developing lateral flow immunoassays [66]. These NPs represent the starting point when this technology is required: the reason might be attributed to their color and the discrimination with respect to the colorless environment. Other reasons are

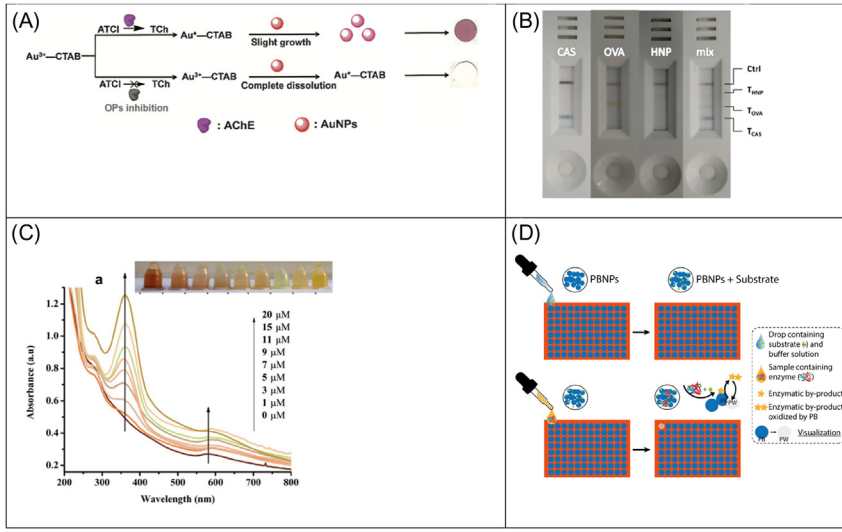


**Figure 13.10** (A) Schematic illustration of colorimetry for the assay of OPs based on the dissolution of AuNPs; (*up*) in the absence of organophosphorous pesticides (OPs), the enzymatic thiocholine (TCh) consumes the $Au^{3+}$ and prevents the dissolution of AuNPs, and (*down*) in the presence of OPs, the enzymatic TCh is not enough to consume all the $Au^{3+}$, and the residual $Au^{3+}$ dissolves the AuNPs [62]. (B) Cross-reaction of the three-colored probes used to label antibodies toward CAS (C-AuNP), HNP (M-AuNP), and OVA (Y-AgNP). The probes were mixed and applied to the YMC multiplex LFIA [63]. (C) Increase in absorbance with increasing concentration of picric acid [64]. (D) Schematic representation of BChE activity visualization, including the enzymatic reaction and the prussian blue (PB) fading [65].

linked to the easiness in conjugation with antibody and/or other species necessary for the lateral flow immunotests, and the low cost. Recently, AuNPs have been integrated into a paper-based immunoassay strip for the detection of uranium in groundwater [67]. The mechanism of the detection is founded on the fact that a monoclonal antibody (clone 12F6) is capable to specifically recognizes U(VI) when complexed to a chelator, the 2,9-dicarboxyl-1,10-phenanthroline (DCP). To reveal U(VI) complex, AuNPs have been conjugated to the antibody and due to the small size of the U-DCP complex, a competitive assay was realized. With this approach, a limit of detection of $\sim$37 nM has been obtained and it should be noted that this result well meets the legal limit of 126 nM set by the WHO and the US EPA for drinking water.

### *13.5.2.2 AgNPs*

As well as for the electrochemical-based detection, the amount of procedures that employ the use of AgNPs to realize colorimetric tests are lower in respect to those based on the use of Au colloids. The main reason is attributable to the starting color

of AgNPs: in fact, differently from the red-based color of AuNPs, the color of AgNPs is usually yellowish. Moreover, the use of AgNPs is reported in literature particularly due to the simplicity in synthesis and to the low cost of the precursors. Recently, Peng et al. developed a method for the detection of ascorbic acid by taking into consideration the growth of AgNPs following a green photo-catalytic route [68]. Briefly, Ag nanoclusters (AgNCs) are obtained by two steps: UV-mediated photosynthesis of NCs with papain and catalytic growth of AgNPs in the presence of ascorbic acid. The difference between the NCs and NPs is in the color; while the former is colorless, the latter is yellow. The NCs represent the catalyst for promoting the synthesis of AgNPs, with an associated change of the plasmon absorption spectra at 420 nm. With this procedure, ascorbic acid has been detected in the range comprised between 0.25 and 50 μM, with a limit of detection as low as ~79 nM (using a spectrophotometer), while the detection limit observed for colorimetric assays taken by the photographs was ~1 μM.

Another approach reported in literature has been consistent with the aggregation of AgNPs for the detection of DNA related to Middle East respiratory syndrome coronavirus (MERS-CoV), *Mycobacterium tuberculosis* (MTB), and human papillomavirus (HPV) [69]. A paper-based multiassay has been developed for using as the detection principle the aggregation of NPs. The AgNPs are stabilized by the citrate ions that give the traditional yellow color. If the cationic PNA probe is not bound to its target, the PNA can interact with the negatively charged AgNPs leading to NP aggregation and a significant color change (from yellow to colorless); instead, a DNA−PNA duplex can be formed when target is present in solution, leading to an electrostatic repulsion of the AgNPs that do not aggregate. Under the optimized condition, the limit of detection for MERS-CoV, MTB, and HPV were found to be 1.53, 1.27, and 1.03 nM, respectively.

However, the yellow color of AgNPs might represents an added value when a multi-chromatic lateral flow assay needs to be developed. The group of Anfossi took advantage of spherical AgNPs, characterized by a brilliant yellow color, to realize a trichromatic lateral flow immunoassay that was capable to detect allergenic proteins, namely casein, ovalbumin, and hazelnut allergenic protein, at levels as low as 0.1 mg $L^{-1}$ [63]. AgNPs were conjugated with anti-ovalbumin antibody, while two different sized (and then differently colored, i.e., red and cyan) AuNPs were conjugated with the anticasein and antihazelnut allergenic protein antibodies. This strategy allowed an obvious identification of the three allergens in commercial biscuits based on the color of the probes; the following three combinations cyan/casein, yellow/ovalbumin, and magenta/hazelnut protein, have been used for visual discrimination (Fig. 13.10B).

### 13.5.2.3 CuNPs and PtNPs

Differently from AuNPs and AgNPs, the making of CuNPs is more challenging because of their easy oxidation, especially when exposed to air or aqueous solution. However, two features make copper suitable in colorimetric analytical tools

development: copper is less expensive than Au and Ag, and the surface plasmon resonance band is similar to AuNPs and AgNPs. In 2016, CuNPs have been produced by using the fatty acid amide *N*-lauryltyramine and hydrazine as capping and reducing agent, respectively [70]. Compared to the other metal-based NPs, the surface plasmon resonance band is centered ~580 nm, and the color of the dispersion appears intense brown. It has been demonstrated how in presence of cysteine (Cys), a color change from brown to olive green is observed. They observed that the color change happened only when both the thiol (SH) and amine ($NH_2$) groups were present in the analyte: CuNPs detected Cys after 2 min while 3 h were necessary to sense L-cysteine ethyl ester (CEE). This behavior can be attributed to the bulkier size of CEE, which may have delayed the contact of SH and $NH_2$ group with CuNPs. The absorbance peak of CuNPs decreased when the Cys concentration increased, displaying a linear range up to 25 μM with a detection limit of 0.1 μM.

Another interesting application of CuNPs has been demonstrated toward the detection of picric acid in real water samples [64]. 30-nm CuNPs have been synthesized by using cefuroxime drug as a protecting agent: the amide group of cefuroxime takes part in coordination with CuNPs, preventing aggregation and acting as capping agent, with the formation of spherical and stable NPs. Authors observed a change in color from red to yellow, supposed to be a consequence of complexation between picric acid and capped-CuNPs: picric acid removes cefuroxime around CuNPs, provoking the aggregation of NPs. The limit of detection was determined to be 38 nM, and the method was capable to provide a linear signal up to a level of 20 μM of picric acid. In addition, the system was evaluated also in presence of species commonly present in aqueous matrices such as pentachlorophenol, 4-nitroanaline, hydroquinone, $Cd^{2+}$, $Ni^{2+}$, $Co^{2+}$, $As^{3+}$, $Cr^{3+}$ and $Hg^{2+}$, but only the presence of picric acid was consistent with color change from red to yellow as shown in Fig. 13.10C.

Among the noble metals, platinum is often used in developing colorimetric assays even if its use in form of NPs is often related to its enzyme-like activity. Chau et al. demonstrated the effectiveness of PtNPs on reduced GO as peroxidase mimetic for the colorimetric detection of specific DNA sequences [71]. In particular, authors took advantage of the synergic combination of PtNPs and graphene: the former is characterized by a peroxidase-like activity, the latter allows stacking interactions with ss-DNA but not with the ds ones. The assay involved the hybridization of a target sequence with its complementary probe sequence, followed by the addition of hybrid nanocomposite PtNPs/rGO. If the concentration of target is low, the nanocomposite is able to bind with the single-stranded probe and it is stabilized against aggregation. After centrifugation, the addition of tetramethylbenzidine (TMB) and hydrogen peroxide leads to an intense blue color. Instead, if the level of target is high, the target/probe duplex can be formed, making the nanocomposite aggregated and thus reducing the recovered PtNPs/rGO after centrifugation; the result is a pale blue production upon the addition of TMB and hydrogen peroxide. The linear range and limit of detection of this assay platform were 0.5−10 and 0.4 nM, respectively.

#### 13.5.2.4 Inorganic nanoparticles

The effectiveness of Prussian Blue is not only visible from an electrochemical point of view, in fact, the role of Prussian Blue in electrocatalyzing the reduction of hydrogen peroxide and the oxidation of thiols is due to a redox couple: Prussian Blue and Prussian White, respectively, the oxidized and the reduced forms. Beyond the electrochemical properties, this material is very interesting because of its change in color between the different oxidation states: when Prussian Blue is reduced to Prussian White, its color changes from blue to colorless. Having in mind this mechanism, Bagheri and colleagues developed the first paper-based multiplatform highlighting the fading of Prussian Blue for sensing the enzymatic activity [65], as reported in Fig. 13.10D. They reported a 96-well chromatographic paper-based platform for the detection of BChE enzyme activity in human serum. Prussian Blue NPs were reagentlessly synthesized within the paper's structure as already reported [65]. The principle of BChE activity detection relies on the reaction between the enzymatic product thiocholine and Prussian Blue. The presence of thiocholine is able to reduce Prussian Blue forming the reduced form, namely Prussian White. The use of a common office scanner was sufficient to detect BChE activity down to 0.8 U $mL^{-1}$ and linearly within a range of 2−15 U $mL^{-1}$.

Another innovative nanomaterial for optical biosensing is Nanoceria, which is a rare-earth oxide nanostructure material, with unique physical and chemical properties compared with that of its bulk material. The $Ce^{3+}/Ce^{4+}$ ratio present in Nanoceria significantly affects its peroxidase-mimetic activity. The combination of this novel material with porphyrin has been evaluated in order to estimate the advantage in adopting a functional molecular material with large conjugated electronic structure. Liu et al. prepared a nanocomposite made with ceria nanorods and 5,10,15,20-tetrakis(4-carboxyl phenyl)-porphyrin ($H_2TCPP$), namely $H_2TCPP-CeO_2$ [72]. This nanocomposite exhibited an intrinsic peroxidase-like activity toward hydrogen peroxide and TMB similarly to horseradish peroxidase enzyme. The combination of these two materials led to a synergistic effect: the electrons can be easily transferred from the conduction band of porphyrin to the conduction band ceria due to the lower level of $CeO_2$ than that of porphyrin. In the presence of glucose oxidase, the reported approach was capable to detect glucose down to $3.3 \times 10^{-5}$ M within a dynamic range between $5.0 \times 10^{-5}$ and $1.0 \times 10^{-4}$ M. However, as for the previous section, the use of this nanocomposite in majority is related to its enzyme-like activity.

Differently from metal NPs, most of the inorganic nanomaterials have been used by taking into advantage their properties of artificial enzymes and they are often combined with coreactant that can change color after some reaction as well as TMB.

## 13.6 Nano/micromotors

Recent trend also includes moving from "classic" substrates to "active" substrate, by the use of self-propelled micro/nanomachines for sensing, which consist of

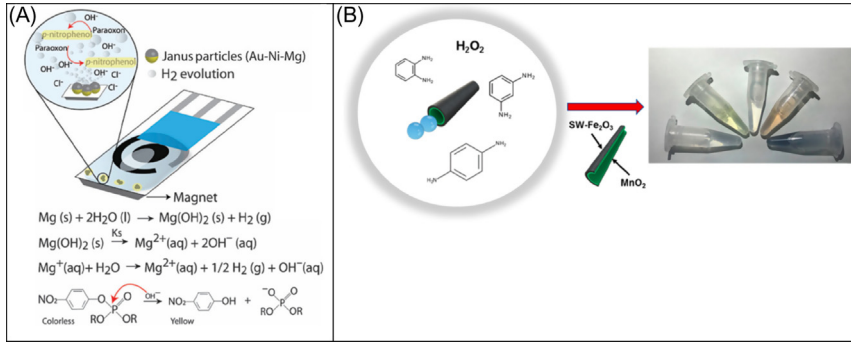


**Figure 13.11** (A) Mechanism and reactions involved in the OP nerve agents degradation to *p*-nitrophenol accelerated by microengines [76]. (B) Schematic of the colorimetric assay with SW − $Fe_2O_3$/$MnO_2$ micromotors for phenylenediamines detection [77].

moving the receptor around the sample, the dimension of those machines ranges from nano to micrometers, and can be fabricated using a wide variety of polymers, metals, and semiconductors [73–75]. In terms of application, they are still at a proof-of-concept stage of tiny objects demonstrating capabilities to autonomously perform different tasks: transporting cargo, destroying cells, remediate pollution. In this direction, the integration of nano/micro entities within electroanalytical and colorimetric devices is highly recommendable. The first combination of micromotors with a SPE has been reported, using Mg-Au-Ni Janus microengines for accelerated destruction of nerve agents, and consequent detection of the non-hazardous remediated product (*p*-nitrophenol) [76]. In this work, smart micromotors were capable of producing $OH^-$ ions to increase the pH of the medium and consequently promote the alkaline degradation of paraoxon into a readily detectable *p*-nitrophenol, Fig. 13.11A. In addition, the produced $H_2$ allowed obtaining a rapid and reproducible nerve-agent degradation with a subsequent detection without the need of external stirrers or mixing devices. The use of microengines leads to a 15-fold increased sensitivity toward organophosphate pesticide detection, compared to a nonengineered SPE. This combined platform represented the first example of an alternative built-in mixing in electroanalysis.

The same principle was successively taken as inspiration by the group of Escarpa, which used an Au-Mg micromotor-based platform for electrochemical detection of diphenyl phthalate in biological and food samples [78]. Also in this case, the increase of pH due to the presence of micromotors, allowed converting diphenyl phthalate into phenol (electroactive molecule). The methodology was applied for direct analysis of phthalate in human plasma, milk, and whiskey, without any sample treatment.

The same group developed a colorimetric method based on the use of tubular micromotors composed of a hybrid SWCNT-$Fe_2O_3$ outer layer and powered by a $MnO_2$ catalyst for the detection and discrimination of phenylenediamine isomers [77] (Fig. 13.11B). In just 15 min, the catalytic decomposition of hydrogen peroxide

(the fuel) caused by the $MnO_2$ catalytic layer resulted in the production of $O_2$ bubbles along with hydroxyl radicals for analytes dimerization. Experimentally, authors observed that *o*-phenylenediamine and *p*-phenylenediamine solutions (500 μM) exhibited strong yellow and pink color, respectively, after 30 min of micromotor's action in presence of 5% $H_2O_2$. A blue solution was obtained when an equimolar mixture of the two isomers was used. The micromotor movement along with radical generation resulted in low limits of detection (5 and 6 μM) and quantification (17 and 20 μM), respectively for *o*-phenylenediamine and *p*-phenylenediamine.

## 13.7 Conclusions

In this chapter, some interesting applications of nanomaterials for the development of analytical devices are presented. The use of nanosized materials belonging from carbonaceous, metallic, or inorganic sources confers to the realized devices improved characteristics of cost-effectiveness, high sensitivity and selectivity, lowest limit of detection, and long-term stability. As illustrated, these NPs are suitable to be combined with each other and/or with different biological elements, producing new nanocomposites always with enhanced performances. Their use also permits for the miniaturization of the platforms, allowing for the realization of wearable devices for the real-time monitoring of physiological parameters. In addition, the miniaturization of platforms paves the way for coupling them with another emerging field: the wearable electronics. The wearable technology market actually shows a very fast growth, being currently worth $30 billion and predicted to rise to $150 billion by 2026, including an expected compound annual growth rate of 32% for wearable chemical sensors for the next 10 years, as stated by the report "Wearable Technology 2016-2026: IDTechEx", June 30, 2016 [79]. In our opinion, this field represents one of the future aspects of the research in sensing devices, which requires a strict synergy between different expertizes such as those of chemical, engineering, materials, and biological areas, boosting the multifarious vision of science.

## Acknowledgments

F.A. and V.S. acknowledge *NanoSWS* project EraNetMed—RQ3-2016 and *AlgaeCB* Bilateral Project Italy-Morocco 2018/2019. F.A. also acknowledges *Nanospes* Project, University of Rome "Tor Vergata" and *Innoconcrete* Project "Con il contributo del Ministero dell'Istruzione dell'Università e della Ricerca della Repubblica Italiana". V.S. also acknowledges *AdSWiM* Interreg Project Italy-Croatia 2019/2020. S.C. acknowledges Marie Skłodowska-Curie Actions Individual Fellowship, this project has received funding from the European Union's Horizon 2020 research and innovation programme under the Marie Skłodowska-Curie grant agreement No 794007.

## References


[1] F. Arduini, S. Cinti, V. Scognamiglio, D. Moscone, G. Palleschi, How cutting-edge technologies impact the design of electrochemical (bio) sensors for environmental analysis. A review, Anal. Chim. Acta 959 (2017) 15−42.

[2] http://graphene-flagship.eu/.

[3] Y. Ito, F. Fukusaki, DNA as a 'nanomaterial', J. Mol. Catal B-Enzym. 28 (2004) 155−166.

[4] A.V. Pinheiro, D. Han, W.N. Shih, H. Yan, Challenges and opportunities for structural DNA nanotechnology, Nat. Nanotechnol. 6 (2011) 763.

[5] J.A. Gerrard, Protein nanotechnology: what is it? Protein Nanotechnology, Humana Press, Totowa, NJ, 2013, pp. 1−15.

[6] https://www.nature.com/collections/vvtzhkzbhm.

[7] F. Arduini, S. Cinti, V. Scognamiglio, D. Moscone, Nanomaterials in electrochemical biosensors for pesticide detection: advances and challenges in food analysis, Microchim. Acta 183 (2016) 2063−2083.

[8] M. Arvand, N. Ghodsi, M.A. Zanjanchi, A new microplatform based on titanium dioxide nanofibers/graphene oxide nanosheets nanocomposite modified screen printed carbon electrode for electrochemical determination of adenine in the presence of guanine, Biosens. Bioelectron. 77 (2016) 837−844.

[9] J. Ping, Y. Wang, Y. Ying, J. Wu, Application of electrochemically reduced graphene oxide on screen-printed ion-selective electrode, Anal. Chem. 84 (2012) 3473−3479.

[10] L. Li, L. Zhang, J. Yu, S. Ge, X. Song, All-graphene composite materials for signal amplification toward ultrasensitive electrochemical immunosensing of tumor marker, Biosens. Bioelectron. 71 (2015) 108−114.

[11] J. Ping, Y. Wang, K. Fan, J. Wu, Y. Ying, Direct electrochemical reduction of graphene oxide on ionic liquid doped screen-printed electrode and its electrochemical biosensing application, Biosens. Bioelectron. 28 (2011) 204−209.

[12] A. Bonanni, C.K. Chua, G. Zhao, Z. Sofer, M. Pumera, Inherently electroactive graphene oxide nanoplatelets as labels for single nucleotide polymorphism detection, ACS Nano 6 (2012) 8546−8551.

[13] E. Morales-Narváez, L. Baptista-Pires, A. Zamora-Gálvez, A. Merkoçi, Graphene-based biosensors: going simple, Adv. Mater. 29 (2017) 1604905.

[14] J. Peña-Bahamonde, H.N. Nguyen, S.K. Fanourakis, D.F. Rodrigues, Recent advances in graphene-based biosensor technology with applications in life sciences, J. Nanobiotechnol. 16 (2018) 75.

[15] S.R. Ryoo, J. Lee, J. Yeo, H.K. Na, Y.K. Kim, H. Jang, et al., Quantitative and multiplexed microRNA sensing in living cells based on peptide nucleic acid and nano graphene oxide (PANGO), ACS Nano 7 (2013) 5882−5891.

[16] E. Morales-Narváez, A.R. Hassan, A. Merkoçi, Graphene oxide as a pathogen-revealing agent: sensing with a digital-like response, Angew. Chem. 125 (2013) 14024−14028.

[17] S. Iijima, Helical microtubules of graphitic carbon, Nature 354 (1991) 56−58.

[18] S. Scognamiglio, Nanotechnology in glucose monitoring: advances and challenges in the last 10 years, Biosens. Bioelectron. 47 (2013) 12−25.

[19] J. Dong, X. Wang, F. Qiao, P. Liu, S. Ai, Highly sensitive electrochemical stripping analysis of methyl parathion at MWCNTs−CeO2−Au nanocomposite modified electrode, Sensor. Actuator. B 186 (2013) 774−780.

[20] H. Huang, T. Chen, X. Liu, H. Ma, Ultrasensitive and simultaneous detection of heavy metal ions based on three-dimensional graphene-CNTs hybrid electrode materials, Anal. Chim. Acta 852 (2014) 45–54.
[21] F.C. Vicentini, B.C. Janegitz, C.M. Brett, O. Fatibello-Filho, Tyrosinase biosensor based on a glassy carbon electrode modified with multi-walled carbon nanotubes and 1-butyl-3-methylimidazolium chloride within a dihexadecylphosphate film, Sens. Actuators B 188 (2013) 1101–1108.
[22] M. Sireesha, V. Jagadeesh Babu, A.S. Kranthi Kiran, S. Ramakrishna, A review on carbon nanotubes in biosensor devices and their applications in medicine, Nanocomposites 4 (2018) 36–57.
[23] S. Kruss, A.J. Hilmer, J. Zhang, N.F. Reuel, B. Mu, M.S. Strano, Carbon nanotubes as optical biomedical sensors, Adv. Drug Deliver. Rev. 65 (2013) 1933–1950.
[24] V. Tjong, H. Yu, A. Hucknall, S. Rangarajan, A. Chilkoti, Amplified on-chip fluorescence detection of DNA hybridization by surface-initiated enzymatic polymerization, Anal. Chem. 83 (2011) 5153–5159.
[25] J.J. Crochet, J.G. Duque, J.H. Werner, S.K. Doorn, Photoluminescence imaging of electronic-impurity-induced exciton quenching in single-walled carbon nanotubes, Nat. Nanotechnol. 7 (2012) 126.
[26] H. Jin, D.A. Heller, M. Kalbacova, J.H. Kim, J. Zhang, A.A. Boghossian, et al., Detection of single-molecule $H_2O_2$ signalling from epidermal growth factor receptor using fluorescent single-walled carbon nanotubes, Nat. Nanotechnol. 5 (2010) 302.
[27] J.H. Kim, D.A. Heller, H. Jin, P.W. Barone, C. Song, J. Zhang, et al., The rational design of nitric oxide selectivity in single-walled carbon nanotube near-infrared fluorescence sensors for biological detection, Nat. Chem. 1 (2009) 473.
[28] Z. Chen, S.M. Tabakman, A.P. Goodwin, M.G. Kattah, D. Daranciang, X. Wang, et al., Protein microarrays with carbon nanotubes as multicolor Raman labels, Nat. Biotechnol. 26 (2008) 1285.
[29] J.H. Kim, J.H. Ahn, P.W. Barone, H. Jin, J. Zhang, D.A. Heller, et al., A luciferase/single-walled carbon nanotube conjugate for near-infrared fluorescent detection of cellular ATP, Angew. Chem. 122 (2010) 1498–1501.
[30] H. Yoon, J.H. Ahn, P.W. Barone, K. Yum, R. Sharma, A.A. Boghossian, et al., Periplasmic binding proteins as optical modulators of single-walled carbon nanotube fluorescence: amplifying a nanoscale actuator, Angew. Chem. 123 (2011) 1868–1871.
[31] J.H. Ahn, J.H. Kim, N.F. Reuel, P.W. Barone, A.A. Boghossian, J. Zhang, et al., Label-free, single protein detection on a near-infrared fluorescent single-walled carbon nanotube/protein microarray fabricated by cell-free synthesis, Nano Lett. 11 (2011) 2743–2752.
[32] F. Arduini, A. Amine, C. Majorani, F. Di Giorgio, D. De Felicis, F. Cataldo, et al., High performance electrochemical sensor based on modified screen-printed electrodes with cost-effective dispersion of nanostructured carbon black, Electrochem. Commun. 12 (2010) 346–350.
[33] F. Arduini, F. Giorgio, A. Amine, F. Cataldo, D. Moscone, G. Palleschi, et al., Electroanalytical characterization of carbon black nanomaterial paste electrode: development of highly sensitive tyrosinase biosensor for catechol detection, Anal. Lett. 43 (2010) 1688–1702.
[34] E.V. Suprun, F. Arduini, D. Moscone, G. Palleschi, V.V. Shumyantseva, A.I. Archakov, Direct electrochemistry of heme proteins on electrodes modified with didodecyldimethyl ammonium bromide and carbon black, Electroanalysis 24 (2012) 1923–1931.

[35] D. Talarico, F. Arduini, A. Constantino, M. Del Carlo, D. Compagnone, D. Moscone, et al., Carbon black as successful screen-printed electrode modifier for phenolic compound detection, Electrochem. Commun. 60 (2015) 78–82.
[36] T.W. Lo, L. Aldous, R.G. Compton, The use of nano-carbon as an alternative to multiwalled carbon nanotubes in modified electrodes for adsorptive stripping voltammetry, Sens. Actuat. B 162 (2012) 361–368.
[37] C.H.A. Wong, A. Ambrosi, M. Pumera, Thermally reduced graphenes exhibiting a close relationship to amorphous carbon, Nanoscale 4 (2012) 4972–4977.
[38] F.C. Vicentini, P.A. Raymundo-Pereira, B.C. Janegitz, S.A. Machado, O. Fatibello-Filho, Nanostructured carbon black for simultaneous sensing in biological fluids, Sens. Actuat. B 227 (2016) 610–618.
[39] R.V. Shamagsumova, D.N. Shurpik, P.L. Padnya, I.I. Stoikov, G.A. Evtugyn, Acetylcholinesterase biosensor for inhibitor measurements based on glassy carbon electrode modified with carbon black and pillar[5]arene, Talanta 144 (2015) 559–568.
[40] S. Cinti, F. Limosani, M. Scarselli, F. Arduini, Magnetic carbon spheres and their derivatives combined with printed electrochemical sensors, Electrochim. Acta 282 (2018) 247–254.
[41] E. Morales-Narváez, B. Pérez-López, L.B. Pires, A. Merkoçi, Simple Förster resonance energy transfer evidence for the ultrahigh quantum dot quenching efficiency by graphene oxide compared to other carbon structures, Carbon 50 (2012) 2987–2993.
[42] Y. Wang, L. Bao, Z. Liu, D.W. Pang, Aptamer biosensor based on fluorescence resonance energy transfer from upconverting phosphors to carbon nanoparticles for thrombin detection in human plasma, Anal. Chem. 83 (2011) 8130–8137.
[43] E. Priyadarshini, N. Pradhan, Gold nanoparticles as efficient sensors in colorimetric detection of toxic metal ions: a review, Sens. Actuat. B 238 (2017) 888–902.
[44] S. Cinti, E. Proietti, F. Casotto, D. Moscone, F. Arduini, Paper-based strips for the electrochemical detection of single and double stranded DNA, Anal. Chem. 90 (2018) 13680–13686.
[45] H. Bagheri, A. Hajian, M. Rezaei, A. Shirzadmehr, Composite of Cu metal nanoparticles-multiwall carbon nanotubes-reduced graphene oxide as a novel and high performance platform of the electrochemical sensor for simultaneous determination of nitrite and nitrate, J. Hazard. Mat. 324 (2017) 762–772.
[46] S. Cinti, R. Cusenza, D. Moscone, F. Arduini, Paper-based synthesis of Prussian Blue nanoparticles for the development of whole blood glucose electrochemical biosensor, Talanta 187 (2018) 59–64.
[47] S. Cinti, S. Politi, D. Moscone, G. Palleschi, F. Arduini, Stripping analysis of As (III) by means of screen-printed electrodes modified with gold nanoparticles and carbon black nanocomposite, Electroanalysis 26 (2014) 931–939.
[48] S. Cinti, F. Santella, D. Moscone, F. Arduini, Hg2 + detection using a disposable and miniaturized screen-printed electrode modified with nanocomposite carbon black and gold nanoparticles, Environ. Sci. Pollut. Res. 23 (2016) 8192–8199.
[49] A. de la Escosura-Muñiz, L. Baptista-Pires, L. Serrano, L. Altet, O. Francino, A. Sánchez, et al., Magnetic bead/gold nanoparticle double-labeled primers for electrochemical detection of isothermal amplified leishmania DNA, Small 12 (2016) 205–213.
[50] J. Huang, Z. Xie, Z. Xie, S. Luo, L. Xie, L. Huang, et al., Silver nanoparticles coated graphene electrochemical sensor for the ultrasensitive analysis of avian influenza virus H7, Anal. Chim. Acta 913 (2016) 121–127.

[51] L. Russo, J. Leva Bueno, J.F. Bergua, M. Costantini, M. Giannetto, V. Puntes, et al., Low-cost strategy for the development of a rapid electrochemical assay for bacteria detection based on AuAg nanoshells, ACS Omega 3 (2018) 18849−18856.
[52] A. Abbaspour, F. Norouz-Sarvestani, A. Noori, N. Soltani, Aptamer-conjugated silver nanoparticles for electrochemical dual-aptamer-based sandwich detection of *Staphylococcus aureus*, Biosens. Bioelectron. 68 (2015) 149−155.
[53] L. Shi, X. Zhu, T. Liu, H. Zhao, M. Lan, Encapsulating Cu nanoparticles into metal-organic frameworks for nonenzymatic glucose sensing, Sens. Actuat. B 227 (2016) 583−590.
[54] P. Ling, J. Lei, L. Jia, H. Ju, Platinum nanoparticles encapsulated metal−organic frameworks for the electrochemical detection of telomerase activity, Chem. Commun. 52 (2016) 1226−1229.
[55] A.A. Karyakin, E.E. Karyakina, L. Gorton, Amperometric biosensor for glutamate using prussian blue-based "artificial peroxidase" as a transducer for hydrogen peroxide, Anal. Chem. 72 (2000) 1720−1723.
[56] S. Cinti, F. Arduini, G. Vellucci, I. Cacciotti, F. Nanni, D. Moscone, Carbon black assisted tailoring of Prussian Blue nanoparticles to tune sensitivity and detection limit towards H2O2 by using screen-printed electrode, Electrochem. Commun. 47 (2014) 63−66.
[57] S. Cinti, M. Basso, D. Moscone, F. Arduini, A paper-based nanomodified electrochemical biosensor for ethanol detection in beers, Anal. Chim. Acta. 960 (2017) 123−130.
[58] S. Cinti, F. Arduini, D. Moscone, G. Palleschi, L. Gonzalez-Macia, A.J. Killard, Cholesterol biosensor based on inkjet-printed Prussian blue nanoparticle-modified screen-printed electrodes, Sens. Actuat. B 221 (2015) 187−190.
[59] S. Cinti, C. Minotti, D. Moscone, G. Palleschi, F. Arduini, Fully integrated ready-to-use paper-based electrochemical biosensor to detect nerve agents, Biosens. Bioelectron. 93 (2017) 46−51.
[60] L. Rivas, C.C. Mayorga-Martinez, D. Quesada-González, A. Zamora-Gálvez, A. de la Escosura-Muñiz, A. Merkoçi, Label-free impedimetric aptasensor for ochratoxin-A detection using iridium oxide nanoparticles, Anal. Chem. 87 (2015) 5167−5172.
[61] Y.S. Nam, K.C. Noh, N.K. Kim, Y. Lee, H.K. Park, K.B. Lee, Sensitive and selective determination of $NO_2^-$ ion in aqueous samples using modified gold nanoparticle as a colorimetric probe, Talanta 125 (2014) 153−158.
[62] S. Wu, D. Li, J. Wang, Y. Zhao, S. Dong, X. Wang, Gold nanoparticles dissolution based colorimetric method for highly sensitive detection of organophosphate pesticides, Sens. Actuat. B 238 (2017) 427−433.
[63] L. Anfossi, F. Di Nardo, A. Russo, S. Cavalera, C. Giovannoli, G. Spano, et al., Silver and gold nanoparticles as multi-chromatic lateral flow assay probes for the detection of food allergens, Anal. Bioanal. Chem. (2018). Available from: https://doi.org/10.1007/s00216-018-1451-6.
[64] M. Hussain, A. Nafady, S.T.H. Sherazi, M.R. Shah, A. Alsalme, M.S. Kalhoro, et al., Cefuroxime derived copper nanoparticles and their application as a colorimetric sensor for trace level detection of picric acid, RSC Adv. 6 (2016) 82882−82889.
[65] N. Bagheri, S. Cinti, V. Caratelli, R. Massoud, M. Saraji, D. Moscone, et al., A 96-well wax printed Prussian Blue paper for the visual determination of cholinesterase activity in human serum, Biosens. Bioelectron. (2019). Available from: https://doi.org/10.1016/j.bios.2019.03.037.
[66] D. Quesada-Gonzalez, A. Merkoci, Nanoparticle-based lateral flow biosensors, Biosens. Bioelectron. 73 (2015) 47−63.

[67] D. Quesada-González, G.A. Jairo, R.C. Blake, D.A. Blake, A. Merkoçi, Uranium (VI) detection in groundwater using a gold nanoparticle/paper-based lateral flow device, Sci. Rep. 8 (2018) 16157.
[68] J. Peng, J. Ling, X.Q. Zhang, L.Y. Zhang, Q.E. Cao, Z.T. Ding, A rapid, sensitive and selective colorimetric method for detection of ascorbic acid, Sens. Actuat. B 221 (2015) 708−716.
[69] P. Teengam, W. Siangproh, A. Tuantranont, T. Vilaivan, O. Chailapakul, C.S. Henry, Multiplex paper-based colorimetric DNA sensor using pyrrolidinyl peptide nucleic acid-induced AgNPs aggregation for detecting MERS-CoV, MTB, and HPV oligonucleotides, Anal. Chem. 89 (2017) 5428−5435.
[70] K.B.A. Ahmed, M. Sengan, S. Kumar, A. Veerappan, Highly selective colorimetric cysteine sensor based on the formation of cysteine layer on copper nanoparticles, Sens. Actuat. B 233 (2016) 431−437.
[71] L.Y. Chau, Q. He, A. Qin, S.P. Yip, T.M. Lee, Platinum nanoparticles on reduced graphene oxide as peroxidase mimetics for the colorimetric detection of specific DNA sequence, J. Mater. Chem. B 4 (2016) 4076−4083.
[72] Q. Liu, Y. Ding, Y. Yang, L. Zhang, L. Sun, P. Chen, et al., Enhanced peroxidase-like activity of porphyrin functionalized ceria nanorods for sensitive and selective colorimetric detection of glucose, Mater. Sci. Eng. C 59 (2016) 445−453.
[73] J. Wang, W. Gao, Nano/microscale motors: biomedical opportunities and challenges, ACS Nano 6 (2012) 5745−5751.
[74] J. Wang, Cargo-towing synthetic nanomachines: towards active transport in microchip devices, Lab Chip 12 (2012) 1944−1950.
[75] W. Wang, W. Duan, S. Ahmed, T.E. Mallouk, A. Sen, Small power: autonomous nano- and micromotors propelled by self-generated gradients, Nano Today 8 (2013) 531−554.
[76] S. Cinti, G. Valdés-Ramírez, W. Gao, J. Li, G. Palleschi, J. Wang, Microengine-assisted electrochemical measurements at printable sensor strips, Chem. Commun. 51 (2015) 8668−8671.
[77] R. María-Hormigos, B. Jurado-Sánchez, A. Escarpa, Self-propelled micromotors for naked-eye detection of phenylenediamines isomers, Anal. Chem. 90 (2018) 9830−9837.
[78] D. Rojas, B. Jurado-Sánchez, A. Escarpa, "Shoot and sense" Janus micromotors-based strategy for the simultaneous degradation and detection of persistent organic pollutants in food and biological samples, Anal. Chem. 88 (2016) 4153−4160.
[79] http://www.idtechex.com/research/reports/wearable-technology-2016-2026-000483.asp.